High-Content Imaging and Gene Expression Approaches To Unravel the Effect of Surface Functionality on Cellular Interactions of Silver Nanoparticles

Bella B. Manshian,[†] Christian Pfeiffer,[‡] Beatriz Pelaz,[‡] Thomas Heimerl,[‡] Marta Gallego,[§] Marco Möller,[§] Pablo del Pino,[§] Uwe Himmelreich,[†] Wolfgang J. Parak,[*,‡,§] and Stefaan J. Soenen[*,†,⊥]

[†]MoSAIC/Biomedical MRI Unit, Department of Medicine, Catholic University of Leuven, Herestraat 49, B3000 Leuven, Belgium, [‡]Physics and Biology Department, Philipps University of Marburg, Renthof 7, D35032 Marburg, Germany, [§]CIC biomaGUNE, San Sebastian 20009, Spain, and [⊥]Biophotonics Group, Faculty of Pharmaceutical Sciences, Ghent University, B9000 Ghent, Belgium

ABSTRACT The toxic effects of Ag nanoparticles (NPs) remain an issue of debate, where the respective contribution of the NPs themselves and of free Ag^+ ions present in the NP stock suspensions and after intracellular NP corrosion are not fully understood. Here, we employ a recently set up methodology based on high-content (HC) imaging combined with high-content gene expression studies to examine the interaction of three types of Ag NPs with identical core sizes, but coated with either mercaptoundecanoic acid (MUA), dodecylamine-modified poly(isobutylene-*alt*-maleic anhydride) (PMA), or poly(ethylene glycol) (PEG)-conjugated PMA with two types of cultured cells (primary human umbilical vein endothelial cells (HUVEC) and murine C17.2 neural progenitor cells). As a control, cells were also exposed to free Ag^+ ions at the same concentration as present in the respective Ag NP stock suspensions. The data reveal clear effects of the NP surface properties on cellular interactions. PEGylation of the NPs significantly reduces their cellular uptake efficiency, whereas MUA-NPs are more prone to agglomeration in complex tissue culture media. PEG-NPs display the lowest levels of toxicity, which is in line with their reduced cell uptake. MUA-NPs display the highest levels of toxicity, caused by autophagy, cell membrane damage, mitochondrial damage, and cytoskeletal deformations. At similar intracellular NP levels, PEG-NPs induce the highest levels of reactive oxygen species (ROS), but do not affect the cell cytoskeleton, in contrast to MUA- and PMA-NPs. Gene expression studies support the findings above, defining autophagy and cell membrane damage-related necrosis as main toxicity pathways. Additionally, immunotoxicity, DNA damage responses, and hypoxia-like toxicity were observed for PMA- and especially MUA-NPs. Together, these data reveal that Ag^+ ions do contribute to Ag NP-associated toxicity, particularly upon intracellular degradation. The different surface properties of the NPs however result in distinct toxicity profiles for the three NPs, indicating clear NP-associated effects.

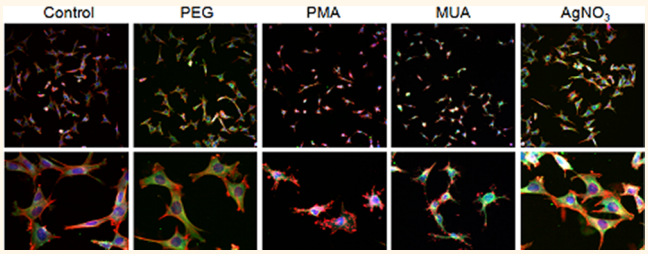

KEYWORDS: silver nanoparticle · nanotoxicology · nanoparticle coating · high-content imaging

The interaction of engineered nanomaterials (NMs) and biological systems such as cells, tissues, or whole organisms is receiving a lot of attention in biomedical research.[1] The potential toxicity of engineered NMs and the remaining uncertainties regarding their safety are slowing down their clinical translation.[2] As the nanotechnology industry holds a lot of potential and hope for important breakthroughs in the fields of therapy and diagnostics for various types of diseases, it is essential that the potential toxicity of NMs is fully characterized in order for these nanotechnologies to fulfill some of their promises. Our current understanding of how NMs interact with biological systems is impeded by various factors which are mainly linked to the lack of standardization in the field.[3] Most studies performed by different research groups use different cell types, assays, and exposure conditions, hindering an easy

* Address correspondence to Wolfgang.Parak@physik.uni-marburg.de, stefaan.soenen@med.kuleuven.be.

Received for review July 27, 2015 and accepted September 1, 2015.

Published online September 01, 2015
10.1021/acsnano.5b04661

comparison between studies. Another reason is the wide variety in different types of NMs with specific physicochemical properties, which are sometimes not adequately characterized. There is therefore still a huge need for combined efforts in the field of nanosafety, where the major points of focus lie upon optimized methodologies, standardization and appropriate NP characterization.[4−6]

A great deal of effort has been applied into optimizing the field of nanosafety, to prepare it for the challenges of the current age and the rapid pace with which the area of nanotechnology itself is developing.[7] The use of high-content (HC) screening strategies has been put forward to enable the generation of large data sets in a limited amount of time[3,8] that can be used in a later stage as source data for bioinformaticians to create predictive models for future, optimized, NP design.[3] A few groups have described HC screening strategies for nanosafety purposes, where the use of zebrafish models has been put forward along with strategies focusing on the viability and oxidative stress in cultured cells.[8−10] As NMs can interact with cultured cells through a variety of mechanisms,[11] the use of more elaborate methodologies that include multiple parameters offers a lot of potential. Additionally, the use of multiple parameters enables the generation of larger databases and will also enhance our understanding of the precise mechanisms involved in how NMs may exert any potential toxicity on cultured cells. Previously, we have established a multiparametric methodology for nanotoxicity studies, where multiple parameters commonly involved in NM toxicity are included.[11] Recently, we have successfully implemented this methodology into a HC imaging screening setup, where the following parameters are included: cell viability, cell membrane damage, oxidative stress, mitochondrial viability, cell morphology and cytoskeleton structure, and induction of autophagy.[12]

In the present study, the HC screening methodology is applied to better understand the effect of silver NPs on cultured cells. Silver NPs, which are known to have a prominent antibacterial effect, also hold a lot of potential for application in biomedical sciences[13] as well as in consumer goods,[14] and have thus been put on the list of most prominent NPs to be tested for nanotoxicity studies by the OECD.[15] There has been some debate whether Ag NPs themselves exert any toxic effects or whether these effects can be solely linked to the level of free Ag^+ ions, due to the fact that disparate data has been published either proving or disproving this hypothesis. Recent studies trying to look into this problem have noticed that the main cause of toxicity of Ag NPs is indeed derived from silver ions, but that the NPs themselves can also further contribute to any toxic effects.[16,17] Many studies on the toxicity of silver NPs have been performed, which have shown that the release of Ag^+ ions from the NPs is a major cause of their toxicity.[16,18,19] From such work it is understood that toxicity of Ag NPs is known to be associated with the level of free Ag^+ ions derived from NP dissolution.[17] This consists both of Ag^+ ions released upon NP dissolution during storage, which increases with time and temperature,[20] as well as intracellular release of Ag^+ ions upon intraendosomal NP dissolution (which has been described to occur 50 times as fast as extracellularly).[21] The rate of silver NP dissolution has been described to be influenced by the precise chemical composition and structure of the Ag core (*i.e.*, considering impurities, different oxidation states of Ag, *etc.*), the nature of the surface coating, and environmental factors such as pH and ionic strength.[22,23] Where the effects of free Ag^+ ions are clear, the contribution of pure NP-related factors remains a topic of discussion.[16,17] Several studies described that silver NP toxicity can be completely linked to the effects of free Ag^+ ions, whereas other studies suggested that the nanoparticulate form of silver presents its own toxic effects.[16] The latter has been ascribed to low levels of free Ag^+ ions in the NP stock suspension,[16] along with the observation that Ag NPs are not that toxic over short time periods due to the relatively slow dissolution of the NPs.[24] It is however important to point out that in equilibrium, due to NPs dissociation, wherever there are Ag NPs, there are also Ag^+ ions,[20,25] which complicates experiments which would allow for distinguishing both effects.

To try and unravel the effect of Ag NPs, we employed three different types of silver NPs (core diameter: 4.2 nm), coated with either mercaptoundecanoic acid (MUA), dodecylamine-modified poly(isobutylene-*alt*-maleic anhydride) (PMA),[26] or poly(ethylene glycol) (PEG)-conjugated PMA.[27] These NPs have already been used in a previous study in which their effect on cell viability has been determined,[28] affirming the high reproducibility of their synthesis. Also their colloidal properties have been fully characterized,[28] enabling us to link toxic effects observed to possible differences in the surface coating of the NPs.[29] To better understand the mechanisms underlying the toxicity of the silver NPs, the HC screening methodology was further supplemented with a detailed analysis of cellular NP uptake along with elaborate gene expression studies and the use of kinetic studies using nonproliferating cell types to understand the impact of NP degradation within the cellular context.

RESULTS AND DISCUSSION

NP Characterization and Integrity. According to previous studies, the diameter of the inorganic Ag NP cores is $d_c = 4.2$ nm, the hydrodynamic diameter d_h of all 3 types of NPs with different surface capping (MUA, PMA, PEG) is around $d_h \approx 11-12$ nm (as determined in water), and all NPs have negative zeta potential.[28] While the PMA and the PEG capped NPs are stable

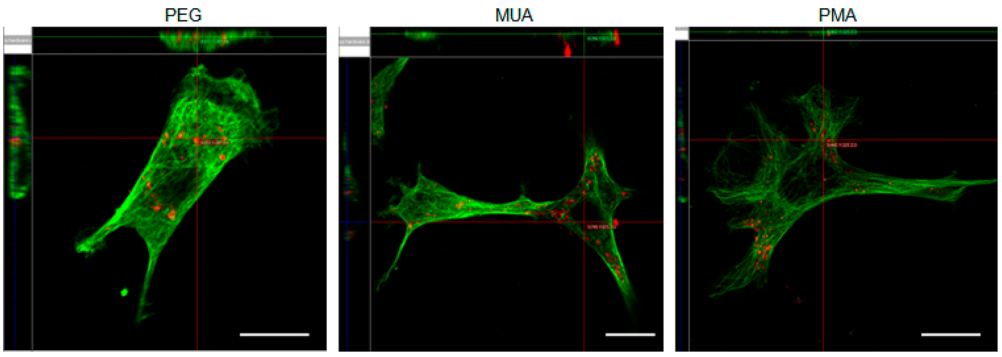

Figure 1. Representative confocal images of HUVEC cells displaying α-tubulin (green) after 24 h incubation with the different silver NPs (red), coated with either PEGylated PMA, MUA, or PMA. These results display clear uptake of all three types of NPs, whereby MUA-coated NPs also show clear cell surface attachment, likely as a result of agglomerated NPs. Scale bars: 50 μm.

even at high NaCl concentrations, the MUA capped NPs were found to agglomerate upon the presence of NaCl.[28] All three NP suspensions were probed to not contain any endotoxins. To understand the effect of NP surface properties on cell toxicity *versus* the effect of dissolved Ag^+, in the present study the level of free Ag^+ ions in the NP stock solutions was measured through inductively coupled plasma mass spectrometry (ICP-MS) to be 102 ± 13, 115 ± 12, and 176 ± 17 μM for PEG-, PMA-, and MUA-coated Ag NPs, respectively (2 μM NP stock suspension in phosphate buffered saline (PBS), corresponding to an Ag concentration of roughly 4.2 mM upon assuming that each Ag NP comprises around 2100 Ag atoms (*cf.* the Supporting Information). These values indicate that the level of free Ag^+ ions in the different samples is quite similar, in plausible agreement with previous studies[23] (*cf.* the Supporting Information), and should thus not cause drastic difference in the level of toxicity caused by Ag^+ ions present in the stock solutions which were added to the cells. As the NPs were used for cell labeling studies, the effect of Ag^+ ions was evaluated by exposing the cells to free Ag^+ ions at (1, 2.5, 5, 10, or 20 μM), equaling the level of free Ag^+ ions present in the stock solutions of PEG-NPs at 20, 50, 100, 200, or 400 nM, respectively; in other words, in our study the effect of solutions of Ag NPs, which contain the Ag NPs, as well as the free Ag^+ ions, which have been released in equilibrium from the Ag NPs in the stock solution upon storage, with the effect of solutions of free Ag^+ ions, which correspond to the concentration of the Ag^+ ions in the stock solution. In our study, we are however not able to distinguish effects from the incorporated Ag NPs, which may arise directly from the Ag NP surface, or from Ag^+ ions that were freshly released once the NPs were located inside endosomal compartments. It also needs to be mentioned that directly administered Ag^+ ions, such as done in this work, will have a different biodistribution than Ag^+ ions which have been released from incorporated Ag NPs.[25]

The dissolution of Ag NPs is strongly pH-dependent, and intracellular dissolution of the NPs will be a key determinant in their toxicological profile, likely more important than the level of free Ag^+ ions present in the original stock suspension. Due to the small size of the NPs, no clear evidence of intracellular NP dissolution could be obtained through electron microscopy (*cf.*, Supporting Information, section V). As the nature of the NP coating may influence the degree of dissolution, this was evaluated in a cell-free manner, where the NPs were exposed to pH 7.5, 6 or 4.6, which correspond to the extracellular, early endosomal, and lysosomal pH levels, respectively.[30] The data shown in the Supporting Information section VI reveal no clear effect of the nature of the NP coating on the extent of degradation, as evaluated by absorbance measurements, ICP-MS of the supernatant, and transmission electron microscopy (TEM) of the NPs themselves.

Cellular NP Uptake. The present study uses two cell types, primary human umbilical vein endothelial cells (HUVEC) and murine C17.2 neural progenitor cells. Both cell types cells have been frequently used by our group for nanotoxicity studies and therefore enable a comparison of results obtained in different studies.[31−33] Primary HUVECs and C17.2 cells also have high biomedical relevance, where they are frequently employed for cell transplantation purposes.[34,35] For this purpose, the cells are often labeled with NPs *in vitro* prior to their transplantation to enable noninvasive monitoring of their migration pattern or as therapeutic entities. For these applications, it is essential that labeled cells do not show any difference to unlabeled cells in their physiological behavior, in order to be able to draw any sound conclusions regarding their biomedical potential.

Understanding the cytotoxic effects of NPs requires detailed knowledge on the initial interactions of these NPs with cultured cells: their level of cell association and cellular internalization. Confocal microscopy of fluorescently tagged NPs reveals clear cell association for all three different types of NPs (Figure 1). The PMA and PEG-NPs show clear internalization of the NPs, where MUA-NPs show both internalization and surface attachment of larger agglomerates. The latter findings

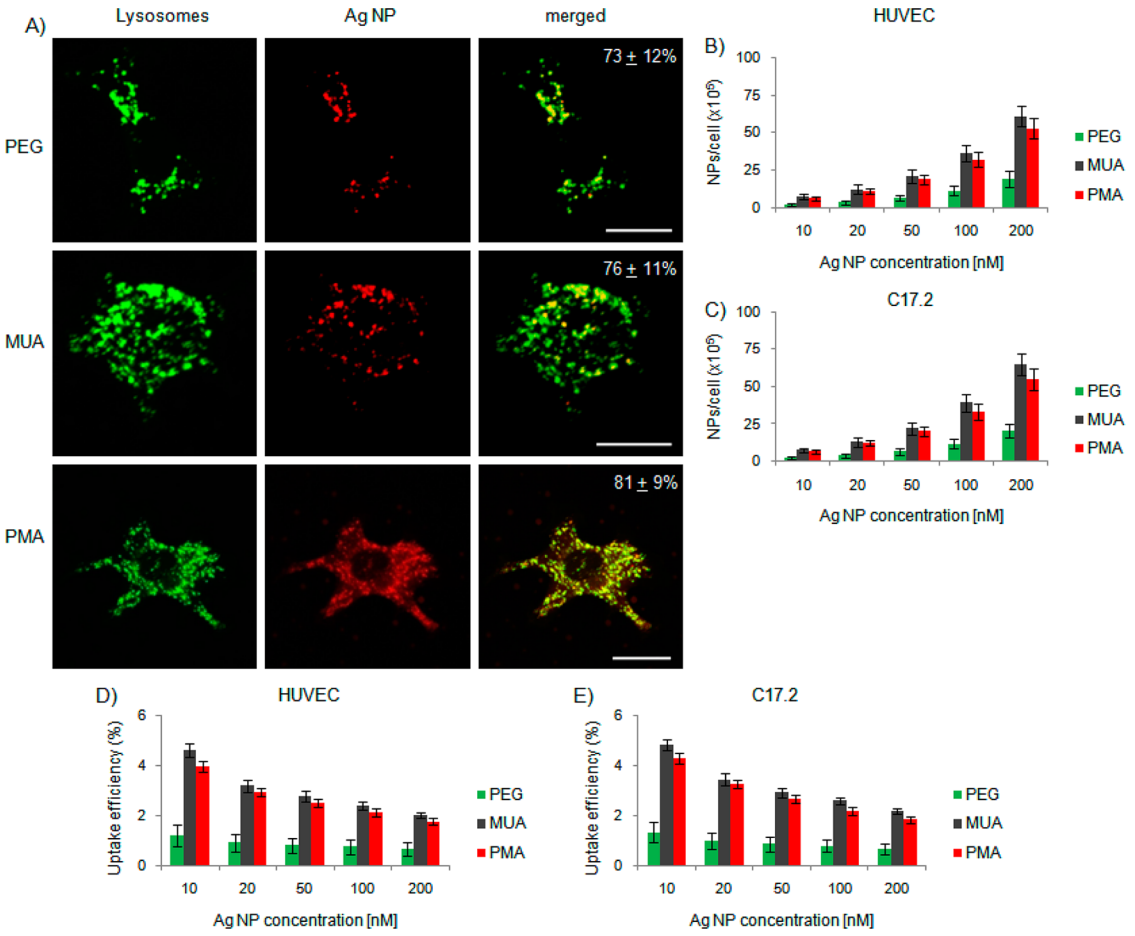

Figure 2. (A) Representative fluorescence microscopy images of cellular uptake of the NPs (red) in C17.2 cells stained for late endosomes/lysosomes (green). The values in the top right corner of the images indicate the level of colocalization of NPs with endosomes/lysosomes expressed as mean ± standard deviation (SD, *n* = 4). Scale bars: 50 μm. Cellular uptake levels (as determined by ICP-MS) for (B) HUVEC and (C) C17.2 cells display concentration-dependent cellular uptake levels. (D and E) Cellular uptake efficiency (*i.e.*, the number of cell-associated NPs over the number of total NPs administered per cell) decreased with NP concentrations in both (D) HUVEC and (E) C17.2 cells, indicating a saturable uptake mechanism, such as endocytosis. The data show that MUA and PMA result in similar levels of cell-associated NPs, whereas PEGylation significantly decreases cell uptake. Data are presented as mean ± standard error of the mean (SEM, *n* = 3).

are in line with previous reports indicating that small surface ligands such as MUA do not provide adequate colloidal stability to the same extent that is achieved upon encapsulation of the NPs in PMA polymers.[36] Upon formation of larger agglomerates, these will sediment onto the cell surface. Previous studies have shown that in NaCl containing media the MUA, but not the PMA- and PEG-NPs, agglomerated.[28]

Additional confocal microscopy was then performed on cells that have been treated with Lysotracker Green for visualization of late endosomes and lysosomes. Figure 2A reveals clear colocalization of all three types of cell-internalized NPs with endosomal compartments, suggesting that the NPs are all internalized by endocytosis, which is in line with literature data.[21] Furthermore, as similar levels of colocalization were observed, this suggests that possible differences in the mechanism of endocytosis do not result in significant differences in intracellular localization of these 3 types of NPs. Please note that for these studies, confocal microscopy was used on a limited number (>10) of cells and any results obtained may therefore not be completely representative for the entire cell population. Supporting Figure VII.1 shows that under the conditions used for imaging, no significant overlap of signals was observed between the different channels, indicating specific signal for either the NPs or lysotracker.

To get quantitative levels of cell-associated NPs, the use of confocal microscopy involves some drawbacks, as due to the optical resolution limit, individual NPs cannot be visualized. Instead, NP-containing endosomes can be counted.[37] Additionally, quantifying fluorescence levels is not without experimental challenges, as differences in the (intra)cellular microenvironment of the NPs (in particular pH) can affect their fluorescence quantum yield,[38] and the efficiency of fluorophore attachment can differ between the different types of NPs, impeding a straightforward comparison.

As all NP cores came from the same batch, they have the same average core size, and therefore, the level of cell-associated NPs was determined by measuring the level of elemental Ag using inductively coupled plasma-mass spectrometry (ICP-MS). For quantitative evaluation, we assumed each Ag NP to comprise 2100 Ag atoms. In this way, by detecting the amount of intracellular Ag, converting this into the number of internalized Ag NPs, and counting the cells, we could be determine the number of Ag NPs associated per cell. Figure 2B,C indicates clear concentration-dependent increases in cellular NP levels, where the level of MUA- and PMA-NPs is substantially higher than the level of PEG-NPs, in agreement with previous qualitative data.[28] These findings are in line with literature data, showing that PEGylation of NPs impedes their cellular uptake by reducing interaction of the NPs with the cell membrane.[39] Additionally, PEGylation will reduce the attachment of serum proteins on the NP surface.[40] As the protein corona is known to play an important role in determining cellular NP uptake mechanisms,[41] the likely changes in protein corona formation on the surface of PEGylated NPs may also affect cellular uptake levels. A more in-depth study of the precise cellular NP uptake mechanisms is however out of the scope of the current study. Importantly, the lower uptake of PEGylated NPs is demonstrated by their lower uptake efficiencies in both cell types (approximately 3.5-fold lower at 10 nM NP concentration) (Figure 2D,E). The data also show a decrease in cellular uptake efficiency for higher NP concentrations (*i.e.*, there is "saturation"), which further supports our previous observation of cellular NP internalization occurring through an active endocytosis mechanism.

Together, these data reveal that PEG-NPs are internalized far less than MUA- or PMA-NPs. MUA- and PMA-NPs show similar levels of cell-association. However, MUA-NPs are more prone to agglomeration and cover the cell surface.

Cell Viability. Cell-NP interactions were studied using high-content (HC) imaging approaches, which generate large data sets for various parameters and where all cellular NP exposure conditions were identical, enabling an easy comparison of results obtained for every parameter. In the present work, several parameters are looked into that have been shown to be important outcomes of NP cytotoxicity.[11] These parameters consist of cell viability, cellular membrane damage, reactive oxygen species (ROS), mitochondrial health, cell spreading, cell skewness, and induction of autophagy. As mentioned above, the influence of free Ag^+ ions already present in the stock solution on cellular wellbeing may not be overlooked. Therefore, cells were exposed to either the Ag NPs at 50, 100, 200, or 400 nM concentration, or to $AgNO_3$ at 2.5, 5, 10, or 20 μM free Ag^+ concentrations, which correspond to the concentration of free Ag^+ present in the Ag NP incubation media at 50, 100, 200, or 400 nM, respectively (*cf.* Supporting Information section II for more detail).

All NPs displayed concentration-dependent cytotoxicity, whereby toxic effects were mostly outspoken for MUA- and PMA-NPs, where significant effects were observed starting from 200 nM (Figure 3A–C). Note that these are relatively high NP concentrations, which are higher than typical NP concentrations used for *in vitro* labeling of cells. The PEG-NPs and $AgNO_3$ from the stock solution only slightly reduced cell viability, not reaching significant effects at NP concentrations up to 400 nM (=20 μM $AgNO_3$). We note again that Ag NP concentrations are not directly comparable with concentrations of ionic silver, as each Ag NP contains ≈2100 Ag atoms, out of which roughly 30% are exposed at the NP surface.[28] Upon NP exposure, the added stock solution contains Ag NPs as well as released Ag^+ ions. Incorporated Ag NPs are located in endosomal/lysosomal compartments (where again they can release Ag^+), whereas the intracellular distribution of administered Ag^+ ions is unclear. For this reason, interpretation of results is not straightforward, and the origin of toxic effects needs to be analyzed in the following. Cells were incubated with diluted Ag NP stock solution, whereby the stock solution contained besides 2 μM NPs also around 100 μM free Ag^+ ions (due to partial NP dissolution in equilibrium in the stock solution), as determined by ICP-MS. In this way, upon exposure in case of an extracellular NP concentration of 400 nM (=2 μM/5), cells are also exposed to 20 μM (100 μM/5, equaling 2.20 μg/mL) free Ag^+ ions. One can now distinguish between the effect of the Ag NPs and the Ag^+ ions in the extracellular solution, as presence of the Ag^+ ions in the extracellular solution can be emulated by exposing cells directly to $AgNO_3$. Exposure of cells to $AgNO_3$ up to 20 μM showed little but nonsignificant reductions of cell viability. With a different cell line, $AgNO_3$ at these concentrations was however found to induce some toxicity.[28] These data suggest that there is a slight cytotoxic effect of the free Ag^+ ions present in the extracellular medium, which originates from partial NP dissolution (already in the stock solution at equilibrium), in line with literature data.[19]

Next to cell viability, the effect of the NPs on cell membrane integrity was also evaluated, revealing clear concentration-dependent membrane damage induced by the MUA-NP, which was much less outspoken for all the other NPs (Figure 3D,E). Ag^+ ions themselves are known to affect lipid membranes and hereby exert cytotoxic effects,[42] yet no significant increase in membrane damage was observed up to 400 nM NP concentration (=20 μM free Ag^+ ($AgNO_3$) concentration). This likely reflects the low level of toxicity caused by free extracellular Ag^+ ions present in the NP suspensions in the culture media, which corresponds with the

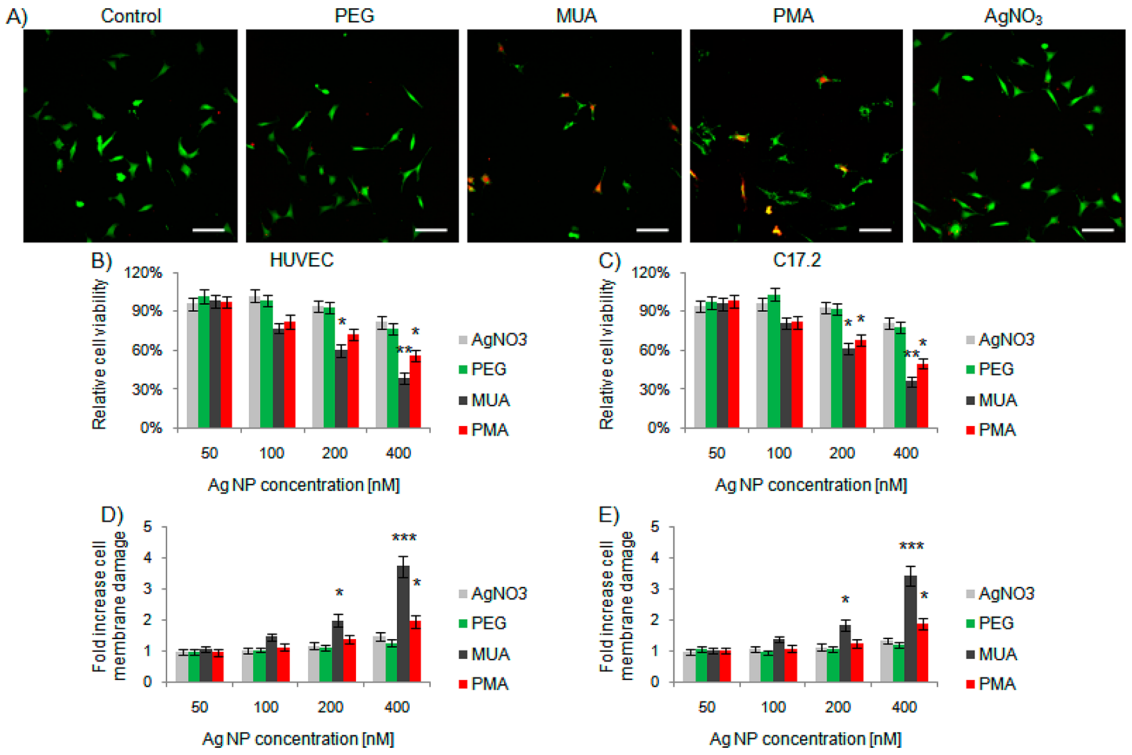

Figure 3. Representative images of C17.2 cells incubated with Ag NPs at 200 nM NP concentration (=10 μM extracellular $AgNO_3$) and stained with calcein-AM (green, live cells) and red dead cell stain (red; dead cells). Scale bars: 200 μm. (B–E) Analysis of high-content imaging indicates clear loss of cell viability in a concentration-dependent manner, which is most outspoken for MUA-coated NPs and PMA-coated NPs in both (B) HUVEC and (C) C17.2 cells. Alternatively, the level of membrane damage of the different NPs increased slightly for all NPs, but was significant for MUA-coated NPs in both (D) HUVEC and (E) C17.2 cells. In (D) and (E), data are expressed as fold-level changes from untreated control cells, where "1-fold" means no effect compared to untreated control cells. These results indicate the effect of NP agglomeration (as noted for MUA NPs) on cell viability, caused by membrane damage. For $AgNO_3$, concentrations of 2.5, 5, 10, and 20 μM were used, equaling the concentration of free Ag^+ present in the NP incubation media at 50, 100, 200, and 400 nM, respectively. Data are presented as mean ± SD for a minimum of 5000 cells per condition. Statistical significance is indicated when appropriate (*$p < 0.05$; **$p < 0.01$; ***$p < 0.001$).

low levels of cytotoxicity of PEG-NPs and $AgNO_3$. The high level of membrane damage for the MUA-NPs likely derives from the high degree of cell surface-attached agglomerates.

Both cell types display similar levels of cytotoxicity and cell membrane damage caused by the NPs. The data obtained reveal high levels of cytotoxicity for PMA-NPs and especially for MUA-NPs. The toxicity of the latter NPs derives, in part, from the formation of agglomerates that sediment on the cell surface, hereby inducing membrane damage.

Effect of NP Degradation on Cell Viability. Upon endosomal uptake of the NPs, the low pH and alterations in salt concentrations can affect degradation kinetics of the NPs, resulting in a more rapid degradation, which is linked to differences in toxicological effects.[31,43,44] Studying the effect of time-dependent NP degradation *in vitro* is quite difficult as cellular NP levels drop rapidly upon cell division, thereby potentially masking effects caused by the degrading NPs. However, most autologous cells *in vivo* do not divide, making them very susceptible to the effects of time-dependent NP degradation. To study this *in vitro*, proliferation-restricted cells were used, which have proven to be useful tools for studying the cytotoxic effects of NP degradation-derived ions in the case of quantum dots and iron oxide NPs.[32,43] In our current study, the data clearly show time-dependent effects of the NPs, which can be attributed to the higher release of Ag^+ ions from internalized NPs. With the use of nontoxic concentrations of the different NPs (at similar intracellular NP levels), a clear increase in cytotoxicity is observed for all three NP types, reaching significant levels after 8 days of incubation (Figure 4). The effect was most outspoken for PMA-NPs, which is in line with their high levels of cell uptake. $AgNO_3$-treated cells did not show any time-dependent effects, indicating that the degradation of the NPs in the endosomes and the high local (endosomal) level of Ag^+ ions induces time-dependent toxicity.

The data obtained are in line with previous studies, where silver NPs were described to exhibit low levels of cytotoxicity on a short time period due to the time required for the dissolution of the NPs.[24] As mentioned before, the dissolution of Ag NPs has been put forward as one of the main causes of toxicity and their antibacterial activity.[45] A recent study by Setyawati *et al.*[22] described how $Ag^{(0)}$ nanoclusters induced higher

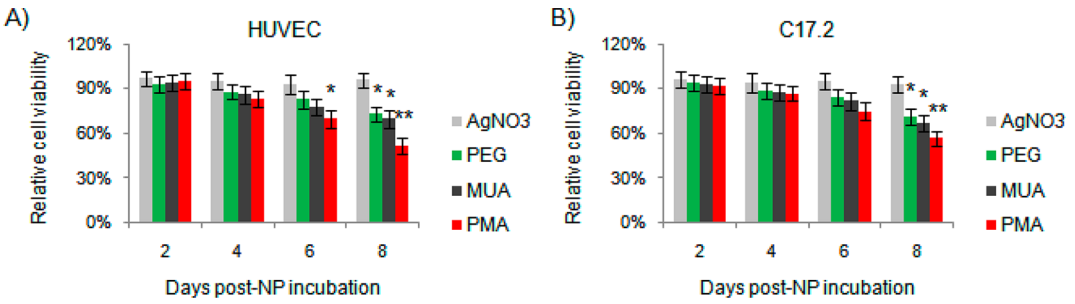

Figure 4. Effects of NP degradation on cell viability. Time-dependent study of cell viability using the Alamar Blue assay on nonproliferating cells. Upon cellular uptake and endosomal enclosure of the NPs, the low endosomal pH may trigger NP degradation and, therefore, release of silver ions. The toxicity of these ions is here measured by determining the viability of nonproliferating cells that have been prelabeled with the NPs at nontoxic concentrations (NP concentration: PEG, 200 nM; MUA and PMA, 50 nM. In the case of $AgNO_3$, a concentration of 10 μM Ag^+ was used, equaling the concentration of free Ag^+ for 200 nM of PEG-NPs). The data clearly show a time-dependent drop in cell viability, which indicates NP degradation. Data are presented as mean ± SEM (n = 3) for a minimum of 5000 cells/condition. Statistical significance is indicated when appropriate (*p < 0.05; **p < 0.01).

toxicity than Ag^+-rich nanoclusters due to the more rapid release of Ag^+ ions in $Ag^{(0)}$ nanoclusters and subsequent oxidation into Ag^+ in the lysosomal compartment. These data indicate that the level of ROS and toxicity can be influenced by the NP core surface. Our findings correlate with previous results suggesting that differences in the surface coating of the NPs have relatively little effect on the intrinsic level of NP dissolution,[28] but that the surface coating will influence cellular NP levels and thereby affect the total level of cellular Ag^+ ions.

Partial dissolution of Ag NPs and associated release of Ag^+ ions did result in low levels of cytotoxicity, as indicated by our findings above where high $AgNO_3$ concentrations (20 μM = concentration of Ag^+ ions present in the highest level of Ag NPs used) induced low cytotoxicity. However, if toxicity were only due to the Ag^+ ions present in the stock solution (*i.e.*, the Ag^+ ions which have been released under equilibrium before the cells were treated with the Ag NPs), the toxicity of all the 3 types of NPs should be similar, as Ag^+ concentrations in the stock solution as determined with ICP-MS are similar. Thus, there must be also an effect depending on the NPs themselves. After cellular uptake, the Ag NPs are located in highly acidic endosomal/lysosomal compartments. Low pH stimulates the release of Ag^+ from Ag NPs. Thus, it is not clear if NP-related cytotoxic effects originate from Ag^+ that is released from the Ag NPs inside endosomal/lysosomal compartments (this "Ag^+" is not the "Ag^+" which was present already in then stock solution), or directly from the undissolved Ag NPs. Regardless of the mechanism, the effect from incorporated NPs is clearly related to the amount of internalized Ag NPs. PEG-NPs are internalized to the lowest extent (*cf.* Figure 2), and have the lowest effect on cell viability (*cf.* Figure 3).

Oxidative Stress. Several studies have shown a substantial effect of Ag NPs on inducing oxidative stress and have linked this with higher levels of cytotoxicity.[46] Here, we tested the effect of the NPs on induction of reactive oxygen species (ROS) and found overall relatively low levels of ROS (Figure 5A–C), only reaching significant increases at 400 nM for PMA-NPs. This low level of ROS is in contrast with most other studies, where the induction of ROS has been put forward as a major cause of Ag NP toxicity.[47] However, as also indicated in several studies, Ag NPs have been found to affect cells through both ROS-dependent and ROS-independent mechanisms,[48] which for the NPs tested here can in part be related to cell membrane damage. Additionally, the use of the HC imaging method together with the CellROX probe provides visual confirmation of the cellular ROS levels. This enables us to assess cellular ROS levels over the entire cell population tested rather than giving an average value for a number of cells tested, as is common for biochemical assays such as the 2′,7′-dichlorodihydrofluoresceindiacetate (H_2DCFDA) assay, which is the most commonly used method. The application of the H_2DCFDA assay in nanotoxicological studies has however been an issue of debate, as its compatibility for NP assays remains questionable.[49] The low levels of cellular ROS may therefore provide a better representation of the NP-induced ROS levels.

Alternatively, ROS may also be more closely associated with specific organelles, such as the mitochondria. Therefore, mitochondrial membrane potential was evaluated (Figure 5A,D,E), revealing a clear loss for cells exposed to the MUA- and PMA-NPs at higher concentrations. The effect of Ag NPs on mitochondrial health is in line with literature data.[47] The specific effect on mitochondria suggest mitochondria-related ROS effects, which are not measured by the cytoplasmic ROS stain and can explain the difference in results for the CellROX and MitoTracker results.

Cell Morphology. Various types of NPs have been shown to affect cellular morphology at subcytotoxic concentrations, resulting in alterations of cytoskeletal-associated cellular signaling pathways, such as cell proliferation, migration, or stem cell differentiation.

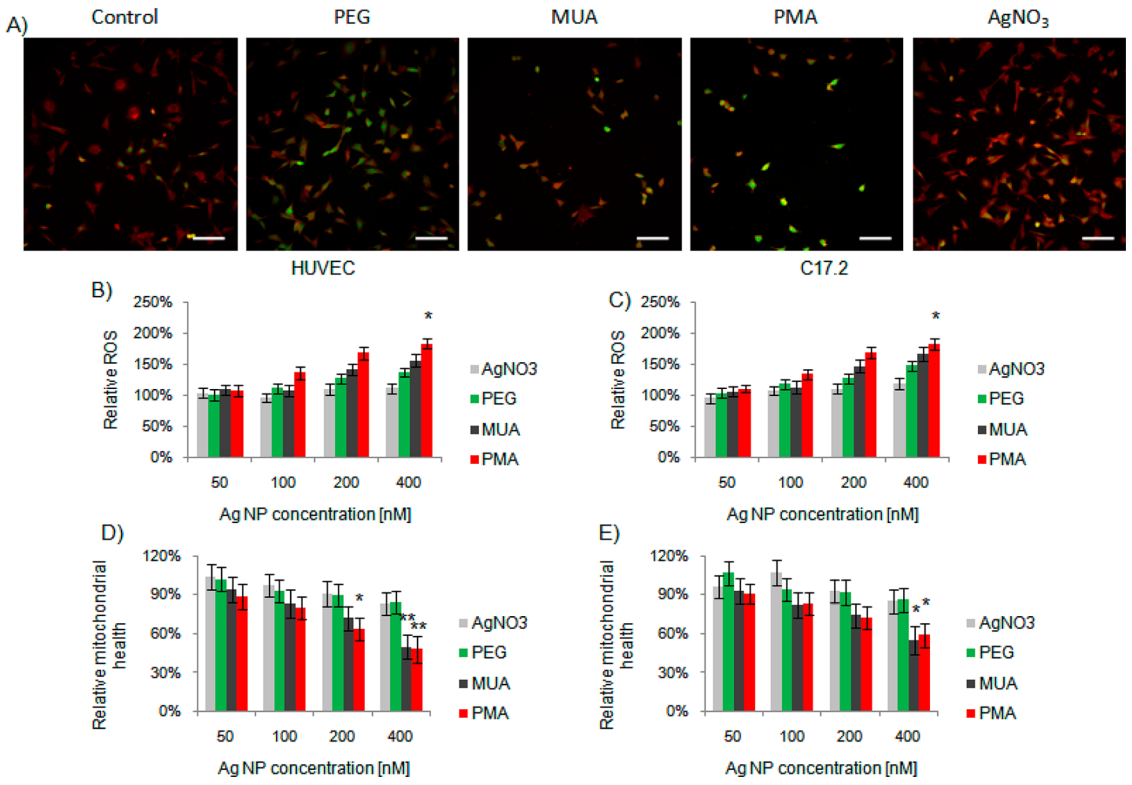

Figure 5. (A) Representative images of C17.2 cells incubated with Ag NPs at 200 nM NP concentration and stained with CellROX green (green, ROS induction) and MitoTracker Red CMXRos (red; mitochondria). Scale bars: 200 μm. (B−E) Analysis of high-content imaging indicates concentration-dependent, but low increases in oxidative stress for PMA-coated NPs and MUA-coated NPs in both (B) HUVEC and (C) C17.2 cells. Alternatively, mitochondrial health was more significantly affected by both PMA- and MUA-coated NPs, in both (D) HUVEC and (E) C17.2 cells. For $AgNO_3$, concentrations of 2.5, 5, 10, and 20 μM were used, equaling the concentration of free Ag^+ present in the NP incubation media at 50, 100, 200, and 400 nM, respectively. Data are presented as mean ± SD for a minimum of 5000 cells per condition. Statistical significance is indicated when appropriate (*$p < 0.05$; **$p < 0.01$).

Assessing the effect of the NPs on cell area and cell skewness at subcytotoxic concentrations enables an easy evaluation of any potential disturbances of the NPs with these important cellular pathways. As high levels of cell death would have affected the outcome of these studies, cells were exposed to the NPs at concentrations up to the level where significant cell death was observed (*i.e.*, from 50 to 400 nM for PEG-NPs and corresponding $AgNO_3$, and 20−200 nM for MUA- and PMA-NPs). The data reveal no effect of the PEG-NPs up to 400 nM (Figure 6A,B), where well-spread cells were observed with clear cytoskeletal structures. Also free $AgNO_3$ up to 20 μM Ag^+ concentrations (equaling the concentration of free Ag^+ in the NP suspensions of 400 nM) did not affect cell morphology. The skewness of the cells (Figure 6D) also indicates no significant changes in the shape of the different cells. On the other hand, both MUA- and PMA-NP affected the cell cytoskeleton, as can be seen from the clear effects on both actin and tubulin fibers (Figure 6A). Analysis of cell spreading shows significant decrease in cell size starting from 100 nM for HUVEC cells and 200 nM for C17.2 cells (Figure 6C). The difference between the two cell types may be related to the difference in total size of the cells, whereby the large HUVEC cells can decrease drastically in size, whereas the smaller C17.2 cells cannot reduce their spreading as effectively. For both cell types, substantial effects could however be observed at subcytotoxic concentrations, indicating that the effect of the Ag NPs on cell cytoskeleton is not a secondary artifact derived from cell death. An increase in cell skewness is also apparent for both types of NPs (Figure 6E), indicating a clear rounding up of the cells. The difference in effects between PEG-NPs, on the one hand, and MUA- and PMA-NPs, on the other hand, indicates that there is a NP specific effect, which is very unlikely to be caused by free Ag^+ ions present in the extracellular medium, but rather should be linked to incorporated NPs. Given the difference between PEG-NPs and MUA- and PMA-NPs, the cytoskeletal deformations are clearly correlated with the (intra)cellular NP levels. This supports our previous hypothesis that cytoskeleton disturbances may be caused by steric hindrance of high levels of endosomes containing rigid and slowly or nondegradable NPs.[50] These findings further support earlier literature data, where Ag NPs were found to result in degeneration of mature neurites in cultures of primary cortical neurons, a process which was linked to a Ag NP-associated reduction in cytoskeletal integrity of treated cells.[51]

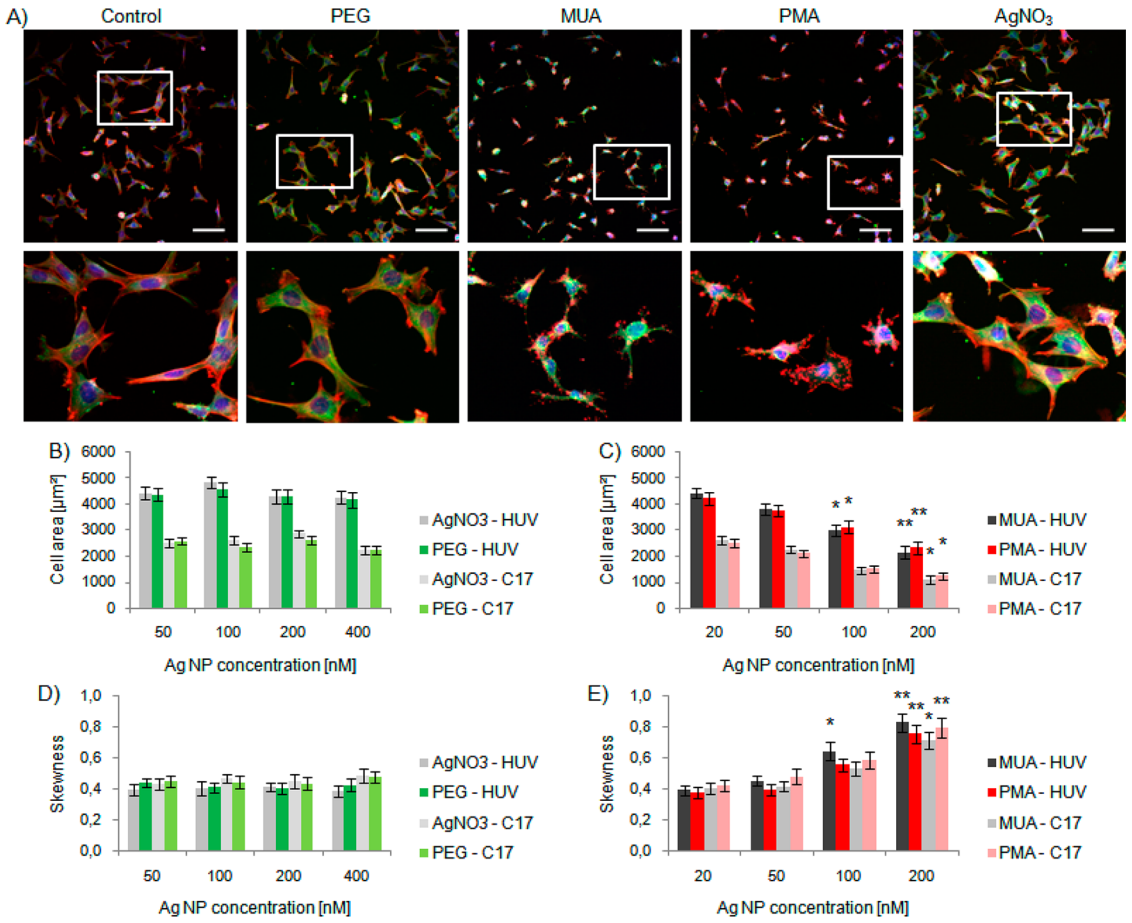

Figure 6. (A) Representative images of C17.2 cells incubated with Ag NPs at 100 nM NP concentration (=5 μM $AgNO_3$) and stained for F-actin (red), α-tubulin (green), and cytoplasm (blue). Scale bars: 200 μm. (B–E) Analysis of high-content imaging indicates no effect of PEG-coated NPs on (B) cell spreading or (D) cell skewness (cell width over cell length). Both MUA and PMA-coated NPs display clear concentration-dependent effects on (C) cell spreading and (E) cell skewness in both cell types, where the cells (at subcytotoxic concentrations) display clear effects on the actin cytoskeleton and result in cell shrinking and cell rounding. For $AgNO_3$, concentrations of 2.5, 5, 10, and 20 μM were used, equaling the concentration of free Ag^+ present in the NP incubation media at 50, 100, 200, and 400 nM, respectively. Data are presented as mean $\pm$ SD for a minimum of 5000 cells per condition. Statistical significance is indicated when appropriate (*$p < 0.05$; **$p < 0.01$).

Autophagy. The induction of autophagy has been suggested to be an important cellular response mechanism of cells to the presence and uptake of foreign substances such as NPs.[52,53] The precise mechanisms by which NPs induce autophagy are diverse and remain the subject of intense research.[53] For slowly or nondegrading NPs, such as gold NPs, the segregation of high levels of NPs into endosomal structures renders these compartments unavailable for normal cellular functionality, thereby reducing the overall cellular degradative capacity. To compensate for this reduced degradation, the cell can stimulate the autophagic pathway. Alternatively, NPs may affect the normal endosomal lumen, such as buffering its pH, and thereby impede the fusion of lysosomes with autophagosomes, which will reduce the normal turnover of the latter compartments.[54] When the internalized NPs damage any organelles, autophagy can also be increased as the normal cellular response to clear away the damaged organelles.[55] Depending on the extent of the autophagy induction, this can either be cytoprotective and help the cell to overcome NP-induced stress,[56] or can result in cell death.[57] A recent study in rats has indicated that Ag NPs can result in hepatotoxicity upon peritoneal injection of the NPs as a direct consequence of Ag NP-induced autophagy.[58]

For the NPs studied in the present work, all NPs have been found to significantly induce autophagy at concentrations of 100 nM for MUA-NPs, 200 nM for PMA-NPs, and 400 nM for PEG-NPs, in contrast to $AgNO_3$, which was found not to have any effect up to 20 μM extracellular Ag^+ concentration (equaling the concentration of free Ag^+ in the NP suspensions of 400 nM) (Figure 7). These data clearly show a clear induction of autophagy for all Ag NPs, which does not appear to be associated with the presence of Ag^+ ions but is a NP-only effect. The high level of autophagy for PMA-and MUA-NPs suggests that autophagy is related to cellular NP levels. However, as the levels of autophagy are higher for MUA-NPs than for PMA-NPs, while

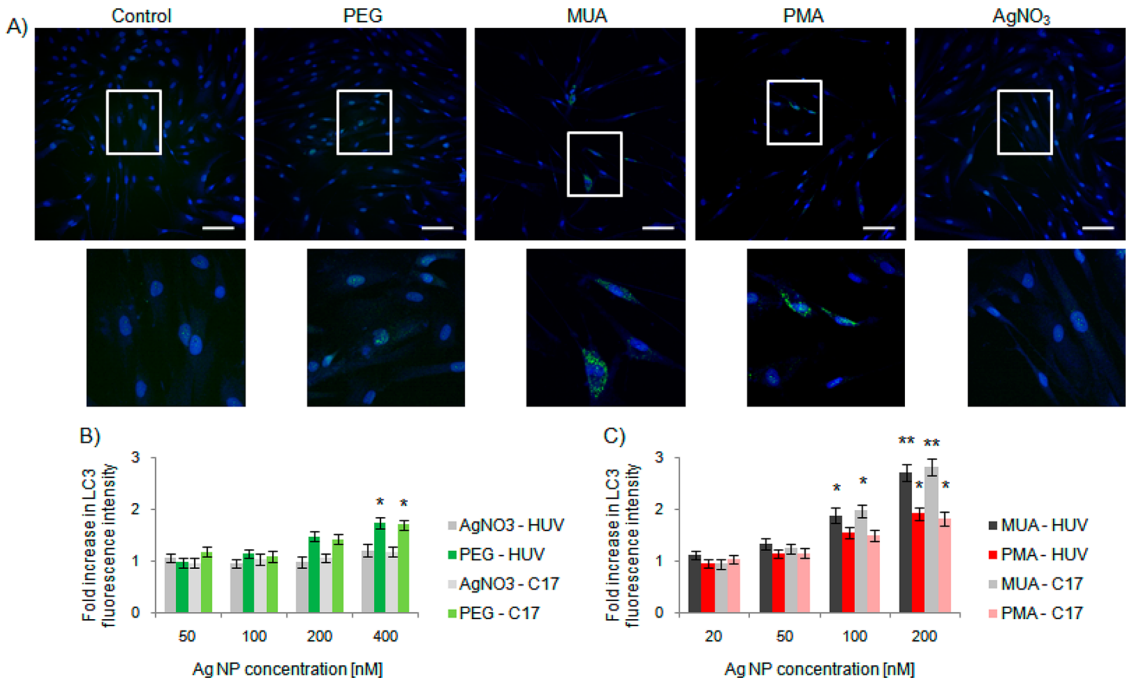

Figure 7. (A) Representative images of C17.2 cells incubated with Ag NPs at 100 nM NP concentrations (=5 μM $AgNO_3$) and stained for LC3 (green, autophagy marker), and nuclei (blue). Scale bars: 200 μm. (B and C) Analysis of high-content imaging reveals concentration-dependent induction of autophagy for all NPs, but most outspoken for MUA- and PMA-coated NPs. No significant induction of autophagy was observed for $AgNO_3$-treated cells. In (D) and (E), data are expressed as fold-level changes from untreated control cells, where "1-fold" means no effect compared to untreated control cells. For $AgNO_3$, concentrations of 2.5, 5, 10, and 20 μM were used, equaling the concentration of free Ag^+ present in the NP incubation media at 50, 100, 200, and 400 nM, respectively. Data are presented as mean ± SD for a minimum of 5000 cells per condition. Statistical significance is indicated when appropriate (*$p < 0.05$; **$p < 0.01$).

the latter have higher levels of intracellular NPs, the colloidal stability of the NPs and the formation and cellular uptake of agglomerates may play an important role in inducing autophagy. The clear induction of autophagy at higher NP levels similar to the level at which NPs induce cytotoxic effects suggests that the high levels of autophagy result in additional cytotoxicity rather than cytoprotection. Where the induction of autophagy by NPs should be avoided for *in vitro* cell labeling experiments, the specific induction of autophagy in tumor cells holds great promise as a future cancer therapy.[57] More research on this particular topic is however warranted, as the NP concentration-dependent effect requires that a specific tumor-associated response would mean that the majority of the NPs end up in the tumor cells. The clear induction of autophagy by the silver NPs studied here in endothelial cells, together with the earlier described silver NP-induced autophagy resulting in hepatotoxicity,[58] suggests that highly efficient targeting approaches are necessary to minimize any undesired side-effects.

Heat Map. The HC imaging studies for the various parameters have revealed that the different Ag NPs affect cultured cells through various mechanisms, including mitochondrial damage, cell membrane damage, induction of autophagy, and disturbing cell cytoskeleton. To easily compare the different NPs, the data of the HC imaging setup can be presented as heat maps[3] (Figure 8). The heat maps show that at similar incubation concentrations (400 nM of Ag NPs or 20 μM of $AgNO_3$), the contribution of free Ag^+ ions in the incubation media does not appear to play a major role in any of the cellular parameters studied, but that most effects observed are clearly NP-related (or due to intracellular NP dissolution). The data reveal that the MUA-NPs are most toxic, especially caused by membrane damage and induction of autophagy, which is likely linked to the formation of agglomerates for these NPs. To probe the intrinsic toxicity of the NPs, regardless of their cellular uptake efficiency, NP effects were compared for PEG-NPs at 200 nM and MUA- and PMA-NPs at 50 nM (rows indicated by black lining on Figure 8).

Here, it shows that at similar cell-associated NP levels, PEG-NPs induced higher levels of ROS and autophagy than the MUA- or PMA-NPs. The effect of PEGylation on ROS induction is in line with previous work on Au NPs, where we observed higher induction of ROS upon PEGylation of Au NPs when comparing cellular effects at similar intracellular NP levels rather than comparing similar incubation doses.[59] PEGylation of the NPs did appear to protect the cells from any cytoskeletal deformations, where effects on cell spreading are nonexisting for PEG-NPs in contrast to MUA- and PMA-NPs.

Expression of Genes Involved in Cellular Stress and Toxicity Responses. Other studies have shown that Ag NPs can

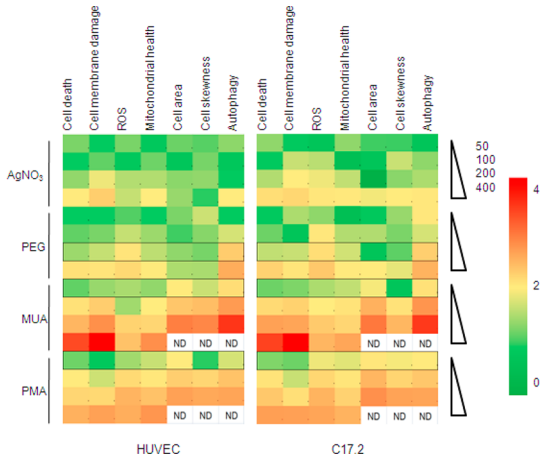

Figure 8. Heat map of the high-content imaging based results for both cell types, where the level of change in the different parameters is indicated as color-code. All data are presented as normalized data relative to the control level, indicating cell death, cell membrane damage, induction of ROS, mitochondrial damage, loss of cell size, cell skewness (cell shape), and induction of autophagy. "ND" stands for Not Determined due to high levels of cell death under these conditions. The concentrations at which similar levels of cell-associated NPs are found are indicated by a dark periphery (PEG, 200 nM; MUA, 50 nM; PMA, 50 nM). For $AgNO_3$, concentrations of 2.5, 5, 10, and 20 μM were used, equaling the concentration of free Ag^+ present in the NP incubation media at 50, 100, 200, and 400 nM, respectively.

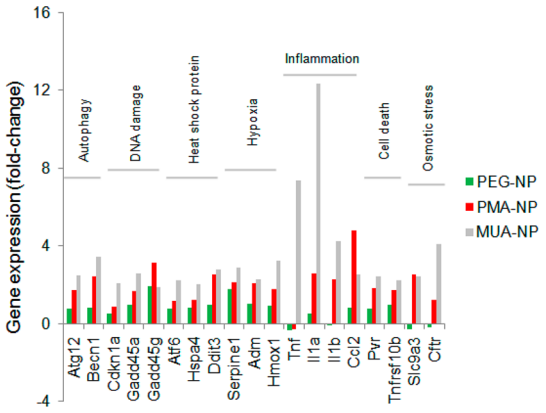

Figure 9. Gene expression of C17.2 cells treated with Ag NPs, where the fold change in gene expression is given for NP-exposed cells compared to control cells only exposed to PBS. From the entire panel of 84 genes tested, only those genes where significant up- or downregulation (2-fold level difference from PBS-treated control cells) was observed are shown.

indeed interact with various signaling pathways.[60] Therefore, to confirm our findings described above and to further unravel the mechanisms by which the different NPs affect cultured cells, gene expression studies were performed on C17.2 cells. For these experiments, the C17.2 cells were selected as they are a stable cell line and gene expression patterns can be reproducibly assessed and easily analyzed. Primary HUVEC cells were omitted from these studies as they come from different individual and thus present a high difference in gene expression patterns between different donors, which impedes a straightforward analysis and does not allow for the experiments to be repeated with a high level of reproducibility. The C17.2 cells were exposed to the different NPs at subtoxic concentrations (100 nM). This low value enabled us to pinpoint those genes of interest and the pathways that will contribute to the onset of cell death, rather than pathways that are activated upon cell death and may only represent a secondary mechanism, not immediately linked to the NPs themselves. Please note that as these studies were performed to elucidate the precise mechanism by which the different NPs affect the cultured cells, no $AgNO_3$-treated samples were included. As all the NP stocks contained similar levels of free Ag^+, any genes specifically regulated by Ag^+ ions would be affected in all three samples. Figure 9 shows an overview of the genes where significant changes (>2-fold change from control) were detected, from a list of 84 genes tested (full table of all genes tested available in the Supporting Information, Table VII.6). The data reveal clear differences between the three NP types, where PEG-NPs did not appear to result in significant changes, compared to PMA-NPs and especially MUA-NPs, where various genes were significantly upregulated. When we look at the various groups of genes, the data reveal that the MUA-NPs affect cells through various mechanisms, even at concentrations where no significant cytotoxicity was observed. The clear differences in gene expression levels between the three different samples also indicate that the genes are affected by the NPs themselves, and not by free Ag^+ ions, as the level of the ions is the same in all three samples. The apparent low contribution of Ag^+ ions on gene expression regulation is in line with another recent study, where it was observed that for rat embryonic cells exposed to Ag NPs and Ag^+ ions, the latter contributed to only 6% of the total number of genes that were affected by Ag NPs.[61]

Slight increases in necrosis-linked genes (Pvr and Tnfrsf10b) were observed, suggesting the MUA-NPs may cause cell death by necrosis. The latter would be explained by the infliction of high levels of cell membrane damage as seen for the MUA-NPs, which would result in necrosis. Also autophagy-specific genes (Atg12 and Becn1) were upregulated, supporting our and previous[58] findings that the NPs induce autophagy and that this is most significant for MUA-NPs. Both PMA- and MUA-NPs resulted in upregulation of Ccl12, Il1a and Il1b, which are linked to inflammation, indicating that Ag NPs likely have immunotoxic effects, which has also been reported in literature.[62] Additionally, effects on genes linked with cell cycle progression (Cdkn1a and Ddit3) were observed for PMA- and MUA-NPs, as well as genes associated with DNA damage (Gadd45a and Gadd45g), suggesting that the NPs

have genotoxic effects. Additionally, several genes associated with hypoxia (Adm, Hmox1 and Serpine1) were upregulated, indicating that the NPs exert hypoxia-like effects on the treated cells. Similar findings have been reported in literature, where tungsten carbide cobalt NPs were found to exert hypoxia-like effects in human skin cells.[63]

Overall, the gene expression studies support our previous findings on the importance of autophagy and cell membrane damage (causing necrosis) as major cell death mechanisms. Additionally, the PMA-NPs and especially the MUA-NPs have been found to induce immunotoxicity, DNA damage and hypoxia. These data reveal the significant differences in the toxic effects of the different Ag NPs, depending on their surface coating. The use of small ligands appears less suited, due to the lower colloidal stability in complex physiological media as many toxic effects appear to be aggravated by the formation of agglomerates.

CONCLUSIONS

The present work illustrates the use of HC imaging technology combined with HC gene expression studies as powerful tools to study the interactions of NPs with cultured cells. The data obtained reveal the importance in surface functionality of the Ag NPs in determining their cellular interactions. Small ligand coated NPs (MUA-NPs) form agglomerates in cell culture media, which sediment on top of the cultured cells. This close interaction of the agglomerates with cultured cells results in cell membrane damage, which kills the cells by necrosis. Additionally, the cellular internalization of agglomerates appears to increase the level of autophagy induction. PMA-coated NPs result in the highest level of cell-internalized NPs and affect cells through autophagy and cytoskeletal deformations, which are clearly linked with intracellular NP amounts. PEGylation of the NPs significantly reduces cellular uptake levels, which overcomes cytoskeletal deformations. However, at similar intracellular NP levels, the induction of ROS is highest for PEG-NPs, suggesting a direct contribution of the PEG chains to the induction of ROS. Exposing the cells to free Ag^+ ions at the same concentration as present in the stock suspension (20 μM of Ag^+ for 400 nM of NPs) reveals that Ag^+ ions do contribute to the toxicity of the NPs, but when present at low levels, the NP-associated effects clearly dominate. Toxicity can be caused by intracellular degradation of the NPs, which release additional Ag^+ ions, especially for slowly or nonproliferating cells. These data prove that apart from toxicity caused by free Ag^+ ions, Ag NPs can affect cells through various mechanisms, the nature and extent of which depend on the surface properties of the NPs.

EXPERIMENTAL SECTION

Nanoparticle Synthesis and Characterization. Ag NPs were synthesized with three different surface coatings (MUA, PMA, PEG) according to the protocol in a previously published study.[28] Also all characterization was performed as described previously.[28]

Cell Culture. C17.2 neural progenitor cells were cultured in high glucose containing Dulbecco's modified Eagle's medium (DMEM), supplemented with 10% fetal calf serum, 5% horse serum, 1 mM sodium pyruvate, 2 mM L-glutamine, and 1% penicillin/streptomycin (Gibco, Invitrogen, Belgium). C17.2 cells were passaged every 48 h and split 1/5. To establish nonproliferating cell cultures, C17.2 cells were exposed with 60 mM Apigenin (Sigma-Aldrich, Bornem, Belgium). As NP uptake is linked with cell cycle progression, Apigenin treatment occurred immediately after cells had been incubated with NPs at the desired concentrations. After media removal, fresh media containing 60 mM Apigenin were used, where 50% of media were replaced every other day with fresh Apigenin-containing medium for the duration of the experiments.

Human umbilical vein endothelial cells (HUVECs) were maintained in endothelial basal/growth culture medium (EBM-2/EGM-2, Clonetics, San Diego, CA) with medium changes every 48 h. Cells were passaged when reaching near 80% confluency by lifting the cells with 0.05% trypsin (Gibco) and were then plated (1/5) onto tissue-culture flasks coated with collagen. To establish nonproliferating HUVEC cultures, cells were given endothelial cell serum-free defined medium (Cell Applications, Tebu-Bio, Le Perray en Yvelines, France) immediately after cells had been exposed to the Ag NPs. Confluent HUVEC monolayers could then be maintained for at least 1 week.

Cell–Nanoparticle Interaction Studies. For HC imaging studies, C17.2 and HUVEC cells were seeded at 5000 cells/well in a 24 well plate (Nunc, Belgium) after which the cells were allowed to attach overnight in a humidified atmosphere at 37 °C and 5% CO_2. Then, the cells were incubated with the different Ag NPs for 24 h in their full growth medium at 50, 100, 200, and 400 nM NP concentration for cell viability and ROS studies, and at 20, 50, 100, and 200 nM for the other studies. As a control, cells were exposed to $AgNO_3$ at 2.5, 5, 10, and 20 μM for 24 h, equaling the amount of free Ag^+ ions in the PEG-NP stock suspensions at 50, 100, 200, and 400 nM, respectively. Every condition was performed in triplicate and results were analyzed based on the three repeats. The HC imaging experiments were then performed as described previously.[12] A full experimental methodology can be found in the Supporting Information that accompanies this manuscript.

Statistical Analysis. All data are expressed as the mean ± standard deviation (SD) unless indicated otherwise. All experiments, except the PCR arrays, were analyzed using the Student's *t*-test. Significance in the PCR arrays was determined based on 2-fold change from the control ΔΔCt value.

Conflict of Interest: The authors declare no competing financial interest.

Acknowledgment. S.J.S. is a post-doctoral fellow from the FWO-Vlaanderen (Fonds voor Wetenschappelijk Onderzoek). Parts of this project were supported by the German Research Foundation (DFG, Grant GRK 1782 to W.J.P.) and the European Commission (Grant FutureNanoNeeds to W.J.P.). B.P. acknowledges the Alexander von Humboldt Foundation for financial support.

Supporting Information Available: The Supporting Information is available free of charge on the ACS Publications website at DOI: 10.1021/acsnano.5b04661.

Additional data on nanoparticle synthesis and characterization, definition of concentrations used, full experimental methodology (PDF)

Note Added after ASAP Publication: This paper posted ASAP on 9/3/15. The surname was corrected for Beatriz Pelaz and the revised version was reposted on 10/7/15.

REFERENCES AND NOTES

1. Maynard, A. D.; Aitken, R. J.; Butz, T.; Colvin, V.; Donaldson, K.; Oberdorster, G.; Philbert, M. A.; Ryan, J.; Seaton, A.; Stone, V.; et al. Safe Handling of Nanotechnology. *Nature* **2006**, *444*, 267–269.
2. Schutz, C. A.; Juillerat-Jeanneret, L.; Mueller, H.; Lynch, I.; Riediker, M.; Consortium, N. Therapeutic Nanoparticles in Clinics and under Clinical Evaluation. *Nanomedicine* **2013**, *8*, 449–467.
3. Nel, A.; Xia, T.; Meng, H.; Wang, X.; Lin, S. J.; Ji, Z. X.; Zhang, H. Y. Nanomaterial Toxicity Testing in the 21st Century: Use of a Predictive Toxicological Approach and High-Throughput Screening. *Acc. Chem. Res.* **2013**, *46*, 607–621.
4. Rivera-Gil, P.; De Aberasturi, D. J.; Wulf, V.; Pelaz, B.; Del Pino, P.; Zhao, Y. Y.; De La Fuente, J. M.; De Larramendi, I. R.; Rojo, T.; Liang, X. J.; Parak, W. J. The Challenge To Relate the Physicochemical Properties of Colloidal Nanoparticles to Their Cytotoxicity. *Acc. Chem. Res.* **2013**, *46*, 743–749.
5. Schrurs, F.; Lison, D. Focusing the Research Effort. *Nat. Nanotechnol.* **2012**, *7*, 546–548.
6. Rivera Gil, P.; Oberdorster, G.; Elder, A.; Puntes, V.; Parak, W. J. Correlating Physico-Chemical with Toxicological Properties of Nanoparticles: The Present and the Future. *ACS Nano* **2010**, *4*, 5527–5531.
7. Joris, F.; Manshian, B. B.; Peynshaert, K.; De Smedt, S. C.; Braeckmans, K.; Soenen, S. J. Assessing Nanoparticle Toxicity in Cell-Based Assays: Influence of Cell Culture Parameters and Optimized Models for Bridging the *in Vitro-in Vivo* Gap. *Chem. Soc. Rev.* **2013**, *42*, 8339–8359.
8. Harris, G.; Palosaari, T.; Magdolenova, Z.; Mennecozzi, M.; Gineste, J. M.; Saavedra, L.; Milcamps, A.; Huk, A.; Collins, A. R.; Dusinska, M.; Whelan, M. Iron Oxide Nanoparticle Toxicity Testing using High Throughput Analysis and High Content Imaging. *Nanotoxicology* **2013**, *9*, 87.
9. George, S.; Xia, T.; Rallo, R.; Zhao, Y.; Ji, Z.; Lin, S.; Wang, X.; Zhang, H.; France, B.; Schoenfeld, D.; et al. Use of a High-Throughput Screening Approach Coupled with *in Vivo* Zebrafish Embryo Screening to Develop Hazard Ranking for Engineered Nanomaterials. *ACS Nano* **2011**, *5*, 1805–1817.
10. George, S.; Pokhrel, S.; Xia, T.; Gilbert, B.; Ji, Z.; Schowalter, M.; Rosenauer, A.; Damoiseaux, R.; Bradley, K. A.; Madler, L.; Nel, A. E. Use of a Rapid Cytotoxicity Screening Approach to Engineer a Safer Zinc Oxide Nanoparticle through Iron Doping. *ACS Nano* **2010**, *4*, 15–29.
11. Soenen, S. J.; Rivera-Gil, P.; Montenegro, J. M.; Parak, W. J.; De Smedt, S. C.; Braeckmans, K. Cellular toxicity of inorganic nanoparticles: Common Aspects and Guidelines for Improved Nanotoxicity Evaluation. *Nano Today* **2011**, *6*, 446–465.
12. Manshian, B. B.; Moyano, D. F.; Rotello, V. M.; Soenen, S. J. High-Content Imaging and Gene Expression Analysis to Study Cell-Nanomaterial Interactions: The Effect of Surface Hydrophobicity. *Biomaterials* **2014**, *35*, 9941–9950.
13. Arvizo, R. R.; Bhattacharyya, S.; Kudgus, R. A.; Giri, K.; Bhattacharya, R.; Mukherjee, P. Intrinsic Therapeutic Applications of Noble Metal Nanoparticles: Past, Present and Future. *Chem. Soc. Rev.* **2012**, *41*, 2943–2970.
14. Faunce, T.; Watal, A. Nanosilver and Global Public Health: International Regulatory Issues. *Nanomedicine* **2010**, *5*, 617–632.
15. Asghari, S.; Johari, S. A.; Lee, J. H.; Kim, Y. S.; Jeon, Y. B.; Choi, H. J.; Moon, M. C.; Yu, I. J. Toxicity of Various Silver Nanoparticles Compared to Silver Ions in Daphnia Magna. *J. Nanobiotechnol.* **2012**, *10*, 14.
16. Beer, C.; Foldbjerg, R.; Hayashi, Y.; Sutherland, D. S.; Autrup, H. Toxicity of Silver Nanoparticles - Nanoparticle or Silver Ion? *Toxicol. Lett.* **2012**, *208*, 286–922.
17. Gliga, A. R.; Skoglund, S.; Wallinder, I. O.; Fadeel, B.; Karlsson, H. L. Size-Dependent Cytotoxicity of Silver Nanoparticles in Human Lung Cells: The Role of Cellular Uptake, Agglomeration and Ag Release. *Part. Fibre Toxicol.* **2014**, *11*, 11.
18. Behra, R.; Sigg, L.; Clift, M. J.; Herzog, F.; Minghetti, M.; Johnston, B.; Petri-Fink, A.; Rothen-Rutishauser, B. Bioavailability of Silver Nanoparticles and Ions: from a Chemical and Biochemical Perspective. *J. R. Soc., Interface* **2013**, *10*, 0396.
19. Foldbjerg, R.; Olesen, P.; Hougaard, M.; Dang, D. A.; Hoffmann, H. J.; Autrup, H. PVP-Coated Silver Nanoparticles and Silver Ions Induce Reactive Oxygen Species, Apoptosis and Necrosis in THP-1 Monocytes. *Toxicol. Lett.* **2009**, *190*, 156–162.
20. Kittler, S.; Greulich, C.; Diendorf, J.; Koller, M.; Epple, M. Toxicity of Silver Nanoparticles Increases during Storage Because of Slow Dissolution under Release of Silver Ions. *Chem. Mater.* **2010**, *22*, 4548–4554.
21. Singh, R. P.; Ramarao, P. Cellular Uptake, Intracellular Trafficking and Cytotoxicity of Silver Nanoparticles. *Toxicol. Lett.* **2012**, *213*, 249–259.
22. Setyawati, M. I.; Yuan, X.; Xie, J.; Leong, D. T. The Influence of Lysosomal Stability of Silver Nanomaterials on Their Toxicity to Human Cells. *Biomaterials* **2014**, *35*, 6707–15.
23. Kim, K. T.; Truong, L.; Wehmas, L.; Tanguay, R. L. Silver Nanoparticle Toxicity in the Embryonic Zebrafish is Governed by Particle Dispersion and Ionic Environment. *Nanotechnology* **2013**, *24*, 115101.
24. Cronholm, P.; Karlsson, H. L.; Hedberg, J.; Lowe, T. A.; Winnberg, L.; Elihn, K.; Wallinder, I. O.; Moller, L. Intracellular Uptake and Toxicity of Ag and CuO Nanoparticles: a Comparison Between Nanoparticles and Their Corresponding Metal Ions. *Small* **2013**, *9*, 970–82.
25. Carillo-Carrion, C.; Nazarenus, M.; Sanchez Paradinas, S.; Carregal-Romero, S.; Almendral, M. J.; Fuentes, M.; Pelaz, B.; del Pino, P.; Hussain, I.; Clift, M. J. D.; et al. Metal Ions in the Context of Nanoparticles towards Biological Applications. *Curr. Opin. Chem. Eng.* **2014**, *4*, 88–96.
26. Zhang, F.; Lees, E.; Amin, F.; Rivera Gil, P.; Yang, F.; Mulvaney, P.; Parak, W. J. Polymer-Coated Nanoparticles: a Universal Tool for Biolabelling Experiments. *Small* **2011**, *7*, 3113–3127.
27. Sperling, R. A.; Pellegrino, T.; Li, J. K.; Chang, W. H.; Parak, W. J. Electrophoretic Separation of Nanoparticles with a Discrete Number of Functional Groups. *Adv. Funct. Mater.* **2006**, *16*, 943–948.
28. Caballero-Diaz, E.; Pfeiffer, C.; Kastl, L.; Rivera-Gil, P.; Simonet, B.; Valcarcel, M.; Jimenez-Lamana, J.; Laborda, F.; Parak, W. J. The Toxicity of Silver Nanoparticles Depends on Their Uptake by Cells and Thus on Their Surface Chemistry. *Part. Part. Syst. Char.* **2013**, *30*, 1079–1085.
29. Chernousova, S.; Epple, M. Silver as Antibacterial Agent: Ion, Nanoparticle, and Metal. *Angew. Chem., Int. Ed.* **2013**, *52*, 1636–1653.
30. Shi, X. L.; Mao, G. J.; Zhang, X. B.; Liu, H. W.; Gong, Y. J.; Wu, Y. X.; Zhou, L. Y.; Zhang, J.; Tan, W. Rhodamine-Based Fluorescent Probe for Direct Bio-Imaging of Lysosomal pH Changes. *Talanta* **2014**, *130*, 356–362.
31. Soenen, S. J.; Demeester, J.; De Smedt, S. C.; Braeckmans, K. The Cytotoxic Effects of Polymer-Coated Quantum Dots and Restrictions for Live Cell Applications. *Biomaterials* **2012**, *33*, 4882–4888.
32. Soenen, S. J. H.; Himmelreich, U.; Nuytten, N.; De Cuyper, M. Cytotoxic Effects of Iron Oxide Nanoparticles and Implications for Safety in Cell Labelling. *Biomaterials* **2011**, *32*, 195–205.
33. Soenen, S. J.; Manshian, B. B.; Himmelreich, U.; Demeester, J.; Braeckmans, K.; De Smedt, S. C. The Performance of Gradient Alloy Quantum Dots in Cell Labeling. *Biomaterials* **2014**, *35*, 7249–7258.
34. Kwon, J. S.; Kim, Y. S.; Cho, A. S.; Cho, H. H.; Kim, J. S.; Hong, M. H.; Jeong, H. Y.; Kang, W. S.; Hwang, K. K.; Bae, J. W. Regulation of MMP/TIMP by HUVEC Transplantation Attenuates Ventricular Remodeling in Response to Myocardial Infarction. *Life Sci.* **2014**, *101*, 15–26.
35. Liang, Y.; Walczak, P.; Bulte, J. W. The Survival of Engrafted Neural Stem Cells within Hyaluronic Acid Hydrogels. *Biomaterials* **2013**, *34*, 5521–5529.

36. Kirchner, C.; Liedl, T.; Kudera, S.; Pellegrino, T.; Munoz Javier, A.; Gaub, H. E.; Stolzle, S.; Fertig, N.; Parak, W. J. Cytotoxicity of Colloidal CdSe and CdSe/ZnS Nanoparticles. *Nano Lett.* **2005**, *5*, 331–338.
37. Rothen-Rutishauser, B.; Kuhn, D. A.; Ali, Z.; Gasser, M.; Amin, F.; Parak, W. J.; Vanhecke, D.; Fink, A.; Gehr, P.; Brandenberger, C. Quantification of Gold Nanoparticle Cell Uptake under Controlled Biological Conditions and Adequate Resolution. *Nanomedicine* **2014**, *9*, 607–621.
38. Soenen, S. J.; Manshian, B.; Doak, S. H.; De Smedt, S. C.; Braeckmans, K. Fluorescent non-porous silica nanoparticles for long-term cell monitoring: Cytotoxicity and particle functionality. *Acta Biomater.* **2013**, *9*, 9183–9193.
39. Martina, M. S.; Nicolas, V.; Wilhelm, C.; Menager, C.; Barratt, G.; Lesieur, S. The *in Vitro* Kinetics of the Interactions between PEG-ylated Magnetic-Fluid-Loaded Liposomes and Macrophages. *Biomaterials* **2007**, *28*, 4143–4153.
40. Pelaz, B.; del Pino, P.; Maffre, P.; Hartmann, R.; Gallego, M.; Rivera-Fernández, S.; de la Fuente, J. M.; Nienhaus, G. U.; Parak, W. J. Surface Functionalization of Nanoparticles with Polyethylene Glycol (PEG): Effects on Protein Adsorption and Cellular Uptake. *ACS Nano* **2015**, *9*, 6996–7008.
41. Walkey, C. D.; Olsen, J. B.; Song, F.; Liu, R.; Guo, H.; Olsen, D. W.; Cohen, Y.; Emili, A.; Chan, W. C. Protein Corona Fingerprinting Predicts the Cellular Interaction of Gold and Silver Nanoparticles. *ACS Nano* **2014**, *8*, 2439–2455.
42. Piao, M. J.; Kang, K. A.; Lee, I. K.; Kim, H. S.; Kim, S.; Choi, J. Y.; Choi, J.; Hyun, J. W. Silver Nanoparticles Induce Oxidative Cell Damage in Human Liver Cells through Inhibition of Reduced Glutathione and Induction of Mitochondria-Involved Apoptosis. *Toxicol. Lett.* **2011**, *201*, 92–100.
43. Soenen, S. J.; Montenegro, J. M.; Abdelmonem, A. M.; Manshian, B. B.; Doak, S. H.; Parak, W. J.; De Smedt, S. C.; Braeckmans, K. The Effect of Nanoparticle Degradation on Poly(methacrylic acid)-Coated Quantum Dot Toxicity: The Importance of Particle Functionality Assessment in Toxicology. *Acta Biomater.* **2014**, *10*, 732–741.
44. Soenen, S. J.; Parak, W. J.; Rejman, J.; Manshian, B. Intra-)Cellular Stability of Inorganic Nanoparticles: Effects on Cytotoxicity, Particle Functionality, and Biomedical Applications. *Chem. Rev.* **2015**, *115*, 2109–2135.
45. Xiu, Z. M.; Zhang, Q. B.; Puppala, H. L.; Colvin, V. L.; Alvarez, P. J. Negligible Particle-Specific Antibacterial Activity of Silver Nanoparticles. *Nano Lett.* **2012**, *12*, 4271–4275.
46. Aueviriyavit, S.; Phummiratch, D.; Maniratanachote, R. Mechanistic Study on the Biological Effects of Silver and Gold nanoparticles in Caco-2 cells--Induction of the Nrf2/HO-1 Pathway by High Concentrations of Silver Nanoparticles. *Toxicol. Lett.* **2014**, *224*, 73–83.
47. Jiang, X.; Foldbjerg, R.; Miclaus, T.; Wang, L.; Singh, R.; Hayashi, Y.; Sutherland, D.; Chen, C.; Autrup, H.; Beer, C. Multi-Platform Genotoxicity Analysis of Silver Nanoparticles in the Model Cell Line CHO-K1. *Toxicol. Lett.* **2013**, *222*, 55–63.
48. Chairuangkitti, P.; Lawanprasert, S.; Roytrakul, S.; Aueviriyavit, S.; Phummiratch, D.; Kulthong, K.; Chanvorachote, P.; Maniratanachote, R. Silver Nanoparticles Induce Toxicity in A549 Cells *via* ROS-Dependent and ROS-Independent Pathways. *Toxicol. In Vitro* **2013**, *27*, 330–338.
49. Hoet, P. H.; Nemery, B.; Napierska, D. Intracellular Oxidative Stress Caused by Nanoparticles: What do we Measure With the Dichlorofluorescein Assay? *Nano Today* **2013**, *8*, 223–227.
50. Soenen, S. J. H.; Nuytten, N.; De Meyer, S. F.; De Smedt, S. C.; De Cuyper, M. High Intracellular Iron Oxide Nanoparticle Concentrations Affect Cellular Cytoskeleton and Focal Adhesion Kinase-Mediated Signaling. *Small* **2010**, *6*, 832–842.
51. Xu, F. L.; Piett, C.; Farkas, S.; Qazzaz, M.; Syed, N. I. Silver Nanoparticles (AgNPs) Cause Degeneration of Cytoskeleton and Disrupt Synaptic Machinery of Cultured Cortical Neurons. *Mol. Brain* **2013**, *6*, 29.
52. Stern, S. T.; Adiseshaiah, P. P.; Crist, R. M. Autophagy and Lysosomal Dysfunction as Emerging Mechanisms of Nanomaterial Toxicity. *Part. Fibre Toxicol.* **2012**, *9*, 20.
53. Peynshaert, K.; Manshian, B. B.; Joris, F.; Braeckmans, K.; De Smedt, S. C.; Demeester, J.; Soenen, S. J. Exploiting Intrinsic Nanoparticle Toxicity: The Pros and Cons of Nanoparticle-Induced Autophagy in Biomedical Research. *Chem. Rev.* **2014**, *114*, 7581–7609.
54. Ma, X.; Wu, Y.; Jin, S.; Tian, Y.; Zhang, X.; Zhao, Y.; Yu, L.; Liang, X. J. Gold Nanoparticles Induce Autophagosome Accumulation through Size-Dependent Nanoparticle Uptake and Lysosome Impairment. *ACS Nano* **2011**, *5*, 8629–8639.
55. Barbour, J. A.; Turner, N. Mitochondrial Stress Signaling Promotes Cellular Adaptations. *Int. J. Cell Biol.* **2014**, *2014*, 156020.
56. Luo, Y. H.; Wu, S. B.; Wei, Y. H.; Chen, Y. C.; Tsai, M. H.; Ho, C. C.; Lin, S. Y.; Yang, C. S.; Lin, P. P. Cadmium-Based Quantum Dot Induced Autophagy Formation for Cell Survival *via* Oxidative Stress. *Chem. Res. Toxicol.* **2013**, *26*, 662–673.
57. Soenen, S. J.; Demeester, J.; De Smedt, S. C.; Braeckmans, K. Turning a Frown Upside Down: Exploiting Nanoparticle Toxicity for Anticancer Therapy. *Nano Today* **2013**, *8*, 121–125.
58. Lee, T. Y.; Liu, M. S.; Huang, L. J.; Lue, S. I.; Lin, L. C.; Kwan, A. L.; Yang, R. C. Bioenergetic Failure Correlates with Autophagy and Apoptosis in Rat Liver following Silver Nanoparticle Intraperitoneally Administration. *Part. Fibre Toxicol.* **2013**, *10*, 40.
59. Soenen, S. J.; Manshian, B. B.; Abdelmonem, A. M.; Montenegro, J. M.; Tan, S.; Balcaen, L.; Vanhaecke, F.; Brisson, A. R.; Parak, W. J.; De Smedt, S. C.; Braeckmans, K. The Cellular Interactions of PEGylated Gold Nanoparticles: Effect of PEGylation on Cellular Uptake and Cytotoxicity. *Part. Part. Syst. Char.* **2014**, *31*, 794–800.
60. Comfort, K. K.; Maurer, E. I.; Braydich-Stolle, L. K.; Hussain, S. M. Interference of Silver, Gold, and Iron Oxide Nanoparticles on Epidermal Growth Factor Signal Transduction in Epithelial Cells. *ACS Nano* **2011**, *5*, 10000–10008.
61. Prasad, R. Y.; McGee, J. K.; Killius, M. G.; Suarez, D. A.; Blackman, C. F.; DeMarini, D. M.; Simmons, S. O. Investigating Oxidative Stress and Inflammatory Responses elicited by Silver Nanoparticles using High-Throughput Reporter Genes in HepG2 Cells: Effect of Size, Surface Coating, and Intracellular Uptake. *Toxicol. In Vitro* **2013**, *27*, 2013–2021.
62. Xu, L.; Shi, C.; Shao, A.; Li, X.; Cheng, X.; Ding, R.; Wu, G.; Chou, L. L. Toxic Responses in Rat Embryonic Cells to Silver Nanoparticles and Released Silver Ions as Analyzed *via* Gene Expression Profiles and Transmission Electron Microscopy. *Nanotoxicology* **2015**, *9*, 513–522.
63. Busch, W.; Kuhnel, D.; Schirmer, K.; Scholz, S. Tungsten Carbide Cobalt Nanoparticles Exert Hypoxia-Like Effects on the Gene Expression Level in Human Keratinocytes. *BMC Genomics* **2010**, *11*, 65.